

1           **The Relationship between Connexin Expression and Gap junction**

2                           **Resistivity in Human Atrial Myocardium**

3  
4           PS Dhillon<sup>1</sup> MRCP PhD, R Chowdhury<sup>1</sup> PhD, P Patel<sup>1</sup> BSc, R Jabr<sup>2</sup> PhD, AU Momin<sup>3</sup>  
5           FRCS, J Vecht<sup>1</sup> FRCS, R Gray<sup>2</sup> PhD, A Shipolini<sup>3</sup> FRCS, CH Fry<sup>2</sup> DSc, NS Peters<sup>1</sup> FRCP.

6  
7           <sup>1</sup> National Heart & Lung Institute, Imperial College, St Mary's Hospital, London.

8           <sup>2</sup> Institute of Biosciences and Medicine, University of Surrey, Guildford, UK.

9           <sup>3</sup> Department of Cardiothoracic Surgery, The London Chest Hospital, London

10  
11           Short title: Atrial connexins, myocardial resistivity and age

12           Supported by The British Heart Foundation grant (FS/03/031/15498 and RG/05/009)

13           Word count: 5298

14           Journal Subject Heads: [132] Arrhythmias-basic studies; [108] Other myocardial biology

15           Correspondence:                   Professor Nicholas S. Peters

16   Waller Cardiac Department

17   St. Mary's Hospital

18   Praed Street

19   London

20   W2 1NY, UK

21   Fax number: +0044 20 7886 1763

22   Telephone number: +0044 20 7886 2468

23   Email: n.peters@imperial.ac.uk

26 **Abstract**

27 *Background:* The relative roles of the gap-junctional proteins connexin40 (Cx40) and  
28 connexin43 (Cx43) in determining human atrial myocardial resistivity is unknown. In  
29 addressing the hypothesis that changing relative expression of Cx40 and Cx43 underlies an  
30 increase in human atrial myocardial resistivity with age, this relationship was investigated by  
31 direct ex-vivo measurement of gap-junctional resistivity and quantitative connexin  
32 immunoblotting and immunohistochemistry.

33 *Methods and Results:* Oil-gap impedance measurements were performed to determine  
34 intracellular resistivity ( $R_i$ ) and gap-junctional resistivity ( $R_j$ ). Total Cx40 quantification by  
35 Western blotting correlated with  $R_i$ , ( $r=0.64$ ,  $p<0.01$ ,  $n=20$ ), and  $R_j$ , ( $r=0.63$ ,  $p=0.01$ ,  $n=20$ ).  
36 Although Cx43 expression showed no correlation with resistivity values, the proportional  
37 expression of the two connexins, ( $Cx40/[Cx40+Cx43]$ ) correlated with  $R_i$  and  $R_j$  ( $r=0.58$ ,  
38  $p<0.01$  for  $R_i$  and  $r=0.51$ ,  $p=0.02$  for  $R_j$ ). Cx40 localised to the intercalated disks was  
39 quantified by confocal immunohistochemical imaging of *en-face* disks, and also correlated  
40 with  $R_j$  ( $r=0.66$ ,  $p=0.02$ ,  $n=12$ ). Advancing age was associated with a rise in  $R_i$  ( $r=0.77$ ,  
41  $p<0.0001$ ),  $R_j$  ( $r=0.65$ ,  $p<0.001$ ,  $n=23$ ), Cx40 quantity ( $r = 0.54$ ,  $p=0.01$ ,  $n=20$ ), and Cx40 gap  
42 junction protein per unit area of *en-face* disk ( $r=0.61$ ,  $p=0.02$ ,  $n=12$ ).

43 *Conclusion:* Cx40 is the main determinant of human right atrial gap-junctional resistivity  
44 such that increased total, gap-junctional and proportional Cx40 expression increases gap-  
45 junctional resistivity. Accordingly, advancing age is associated with an increase in Cx40  
46 expression and a corresponding increase in gap-junctional resistivity. These findings are the  
47 first to demonstrate this relationship and a mechanistic explanation for changing atrial  
48 conduction and age-related arrhythmic tendency.

49

50 **Keywords:** Gap junction, Connexin, Conduction, Arrhythmogenesis

## 51 **Introduction**

52 Gap-junction (GJ) channels are transmembrane proteins that in myocardium mediate cell-to-  
53 cell coupling required for ordered action potential (AP) propagation.<sup>1-3</sup> Each GJ channel is  
54 formed from two hemi-channels (connexons), in-turn composed of six connexin (Cx) subunit  
55 proteins. In the human atrium Cx40 and Cx43 are the major connexins, with small amounts  
56 of a third, Cx45, also expressed.<sup>1-4</sup>

57 The relative contributions of Cx40 and Cx43 in determining atrial conduction properties has  
58 been investigated in murine Cx-gene knock-out models, which suggested that reduction of  
59 Cx40 slowed conduction, and prolonged P-waves, whereas reduction of Cx43 had little  
60 effect.<sup>5-7</sup> In a human open-chested mapping study, conduction velocity (CV) during sinus  
61 rhythm and atrial pacing was correlated with Cx40 and Cx43 in matched tissue samples.<sup>8</sup> In  
62 contrast to the murine studies, CV was reduced as the proportion of Cx40 signal increased  
63 (and therefore that of Cx43 decreased). Consistent with these findings, a study using  
64 synthetic strands of neonatal and foetal murine atrial cardiomyocytes showed that Cx40  
65 deletion (Cx40<sup>-/-</sup>) was associated with increased CV, and genetic deletion of Cx43 (Cx43<sup>-/-</sup>)  
66 was associated with a decrease of CV.<sup>9</sup> In light of these apparently conflicting results, and  
67 given the importance of a mechanistic understanding of this relationship specifically in  
68 humans, we investigated the relationship between human atrial connexin expression and gap-  
69 junctional resistance, the key intermediary and gap-junctional determinant of myocardial  
70 conduction velocity. Biophysical theory proposes that an increase of gap-junctional  
71 resistance ( $R_j$ ) reduces CV.<sup>10</sup>

72 We used the validated method of myocardial oil-gap impedance measurements,<sup>11</sup> to measure  
73  $R_j$ , and in the same human myocardial samples used quantitative Cx40 and Cx43  
74 immunoblotting and immunohistochemistry, to address the hypotheses that there is a  
75 relationship between the relative expression of Cx40 and Cx43 and  $R_j$ , and that changes in the

76 relative expression of Cx40 and Cx43 underlie an increasing atrial myocardial resistivity with  
77 age.

78

## 79 **Patients and Methods**

80 *Specimen source, collection and handling.* The use of human tissue conformed to the  
81 principles outlined in the Declaration of Helsinki and the study had local Ethical Committee  
82 approval with written informed consent. Atrial appendage biopsies were collected from  
83 patients undergoing cardiac surgery at The London Chest Hospital, London, UK. Twenty-  
84 three patients (15M) in sinus rhythm (age  $68\pm 8$  years, range 53-80 years) undergoing  
85 coronary bypass surgery (CABG, n=15), aortic valve replacement (AVR, n=3) or both (n=5)  
86 were included. Patients were in sinus rhythm at the time of surgery as assessed by ECG and  
87 did not have any history of atrial arrhythmia. All patients underwent surgery using  
88 conventional cardiopulmonary bypass support, and biopsies were collected from the tips of  
89 the right atrial appendage immediately after the pericardium was opened and prior to  
90 exposure to cardioplegic agents. Samples were divided immediately upon collection; one part  
91 was snap-frozen in liquid nitrogen at  $-70^{\circ}\text{C}$  for subsequent Cx quantification and  
92 immunolabelling, and the remainder was transported to the laboratory in pre-oxygenated  
93 Tyrode's solution ( $4^{\circ}\text{C}$ ) containing (mM) NaCl 118, KCl 4.0,  $\text{NaHCO}_3$  24,  $\text{NaH}_2\text{PO}_4$  0.4,  
94  $\text{MgCl}_2$  1.8, glucose 6.1, Na pyruvate 5.0 (pre-gassed with 95% $\text{O}_2$ /5% $\text{CO}_2$ , pH  $7.35 \pm 0.03$ ).  
95 Transportation time to the laboratory was approximately 15 minutes. On arrival at the  
96 laboratory the unfrozen specimens were gradually warmed to  $37^{\circ}\text{C}$  and atrial trabeculae were  
97 dissected for physiological experiments. This approach permitted extraction of connexin  
98 protein for Western blotting, and parallel determination of gap junction resistance in intact  
99 myocardium. All chemicals were from Sigma, UK.

100

101 *Measurements of longitudinal impedance and calculation of gap junction resistance.* The  
102 method and its validation have previously been described in detail<sup>11</sup> and are available in our  
103 online supplement. Myocardial preparations ( $\leq 1$  mm diam. 5-6 mm length) were placed in a  
104 three-chambered bath; the outer chambers were superfused with Tyrode's solution at 37°C,  
105 whilst the muscle in the central chamber was coated with mineral-oil gel. Myocardial strips  
106 have been shown to remain metabolically and structurally intact during impedance  
107 measurements.<sup>11,11a</sup> Alternating current (0.25-150 kHz) was passed between platinum (Pt)-  
108 black electrodes in the outer chambers to constrain current to the intracellular pathway of the  
109 muscle within the oil-gap, with a fraction through a parallel extracellular shunt. The  
110 frequency-dependent intracellular resistance ( $r$ ) of the preparation was recorded with a  
111 balanced Wien bridge (Wayne-Kerr, Wetherby, UK). Total preparation impedance,  $z$ , was  
112 modelled as  $z = (z_i \cdot r_{ec}) / (z_i + r_{ec})$ , where  $r_{ec}$  is the resistance of the extracellular shunt and  $z_i$  is  
113 the impedance of the intracellular pathway.  $r_{ec}$ , was measured separately as the resistance  
114 between two Pt-black needle electrodes, a known distance apart, placed in the muscle within  
115 the oil-gap to obtain true intracellular resistance,  $r_i$ , from  $r_i = (r \cdot r_{ec}) / (r + r_{ec})$ . Intracellular  
116 resistance itself has two components; the sarcoplasm,  $r_c$ , and gap junction resistances,  $r_j$ , (i.e.  
117  $r_i = r_j + r_c$ ), obtained separately by measuring the frequency-dependent component of  $r_i$  and the  
118 limiting value at high frequencies (Figure 1). Preparation length and radius in the oil-gap  
119 were measured after measurements. Lower case values of variables ( $r, x; \Omega \cdot \text{cm}^{-1}$ ) were  
120 converted to specific ( $R, X; \Omega \cdot \text{cm}$ ) values by scaling to preparation cross-section area (CSA)  
121 and the proportion of CSA occupied by muscle. The non-muscle fraction of CSA was  
122 calculated from the value of  $r_{ec}$ , assuming it was filled with Tyrode's ( $49 \Omega \cdot \text{cm}$ ).<sup>11</sup>

123 *FIGURE 1 NEAR HERE*

124

125 *Connexin protein quantification by Western blotting.* Tissue homogenates were prepared  
126 from frozen tissue samples to give a solution of final concentration 0.5 mg/ml in sample  
127 buffer. Total protein (5.0 mg) from each sample was resolved  
128 ed by polyacrylamide gel electrophoresis (BioRad, Hercules, USA) on a 12.5% gel (4.5%  
129 stacker). The gel was run at 60 V until the dye front was through the stacker and subsequently  
130 run at 150 V. The gel was electrophoretically transferred onto a polyvinylidene fluoride  
131 membrane at constant voltage, 30 V. The membrane was blocked in the dilution buffer (TBS  
132 / 0.1% Tween20 [Merck, UK] / 1% blot qualified BSA / 4% Marvel) for one hour, followed  
133 by incubation with the primary antibody for Cx43 and Cx40 for 1 hour.

134

135 For Cx43, an IgG<sub>1</sub> raised in mice against a synthetic peptide corresponding to positions 252-  
136 270 of rat native Cx43 was used (Chemicon, USA; 1:500 in dilution buffer). For Cx40, a  
137 goat antibody raised against a human peptide mapping near the C-terminus of Cx40 was used  
138 (Santa Cruz Biotechnology, USA; 1:1000 in dilution buffer). Membranes were washed and  
139 incubated for one hour with secondary alkaline phosphatase conjugated anti-mouse for Cx43  
140 and anti-goat for Cx40 (Pierce, Rockford, IL, USA; 1:2,500 dilution. The membrane was then  
141 incubated with alkaline phosphate buffer (0.1 M TRIS pH 9.5, 0.1 M NaCl, 5 mM MgCl<sub>2</sub>),  
142 followed by incubation with freshly prepared Nitro blue tetrazolium chloride (NBT)/ 5-  
143 Bromo-4-chloro-3-indolyl phosphate, toluidine salt (BCIP) substrate solution (Promega  
144 Corp., Madison, WI, USA). Band intensities were quantified by a densitometric scan and all  
145 values corrected for protein loading using the actin band on a coomassie-stained gel run in  
146 parallel. For connexin quantification, one patient was randomly selected and arbitrarily  
147 scored as 100 units of Cx40 and Cx43 and all other values were scaled accordingly.

148

149 *Immunofluorescence confocal microscopy.* Frozen sections (10  $\mu\text{m}$ ) were mounted onto  
150 poly-L-lysine coated slides, fixed in 100% methanol at  $-20^{\circ}\text{C}$  and washed with phosphate  
151 buffered saline before blocking in 1% bovine serum albumin (BSA) for 30 minutes (for  
152 Cx43) or 1hr (for Cx40). The same primary Cx43 and Cx40 antibodies were used as for  
153 protein quantification. Incubation was at a 1:1000 dilution in BSA for 2 hours for both  
154 antibodies. After washing, a secondary antibody tagged with Cy3 fluorescent marker  
155 (Chemicon, USA) for Cx43 and FITC (Chemicon, USA) for Cx40 were used at a dilution of  
156 1:500 and 1:50 respectively in BSA for 45 minutes. Sections were then washed and mounted  
157 with Vectasheild mountant (Vector Labs, CA). Immunolabelled sections were examined  
158 using a Zeiss LSM-780 confocal microscope.

159

160 To assess the degree of connexin lateralization, a previously published, blinded,  
161 semiquantitative visual method was used.<sup>12</sup> A simple, arbitrary score was derived as follows,  
162 based on the degree of clustering of immunolabeled gap junction. Longitudinal orientation by  
163 standard light microscopy of an adjacent section was first confirmed. Immunolabeled  
164 sections were then examined using phase-contrast transmission microscopy, coupled with  
165 fluorescence microscope settings that maintained cell outline visualization to further confirm  
166 longitudinal cell orientation, to assess the distribution pattern of immunolabeled gap  
167 junctions. Three randomly selected optical fields ( $\sim 250,000 \mu\text{m}^2$ ) of at least three separate  
168 tissue sections from each specimen were examined by a single experienced  
169 immunofluorescence microscopist blinded to the origin of the specimens. The scoring system  
170 assessed Cx40 and Cx43 label distribution, ranging from being confined exclusively to the  
171 normal, transversely orientated clusters at cell abutments (score 1), to a distribution of  
172 labelling within longitudinal arrays along the length of the myocyte, with markedly  
173 diminished labelling at the end-on abutments (score 5). Although only semi-quantitative, this

174 technique has proven useful,<sup>12</sup> and identifies changes that are relatively gross and of likely  
175 biological significance.

176

177 *Measurement of connexin expression per unit area per en-face intercalated disc area*

178 Transversely sectioned samples labelled with Cx40 were examined using a Zeiss LSM-780  
179 confocal microscope. 15-to-20 *en-face* discs per patient were selected from at least five  
180 randomly selected fields (230  $\mu\text{m}$  x 230  $\mu\text{m}$ ). Confocal images were converted into TIFF  
181 format using Fiji software and then analysed with Photoshop CS3 (Adobe) software.  
182 Immunolabelled pixels were counted electronically to allow measurement of both intercalated  
183 disc area and Cx40 area per *en-face* disk.

184

185 *Measurement of connexin40 heterogeneity*

186 For each sample, six randomly selected areas (230  $\mu\text{m}$  x 230  $\mu\text{m}$ ) were imaged on a Zeiss LSM-  
187 780 confocal microscope. Using Photoshop CS3 (Adobe) a grid of 7x7 squares was super-  
188 imposed on the image. The number of squares without label was counted and divided by the total  
189 number of squares to give percentage labelled fields as a marker of Cx40 heterogeneity.

190

191 *Quantification of myocardial fibrosis.* Elastin and collagen autofluorescence were measured  
192 with an argon ion laser at 488 nm.<sup>13</sup> 10 $\mu\text{m}$  frozen tissue sections were fixed and mounted at -  
193 20 $^{\circ}\text{C}$  as above and imaged using a confocal microscope (Zeiss Pascal). Quantification used  
194 the ImageJ programme (National Institute of Health) to calculate percentage fluorescence in  
195 six randomly chosen fields per sample.

196

197 *Statistics.* Data are presented as mean $\pm$ SD. Comparisons between groups was performed  
198 with Student's t-test. Association between variables was analysed by Pearson's correlation



199 tests. A one-sided Spearman's rank correlation co-efficient,  $r_s$ , expressed the association  
200 between variables, with no assumed relationship. The null hypothesis was rejected at  $p < 0.05$ .  
201 Impedance data were fitted to the equation of a circle using the program KaleidaGraph  
202 (Synergy Software). All other analysis was performed using Graphpad Prism 2.01 (Graphpad  
203 software).

204

205

206

207

208

209

210

211

212

213 **Results**

214 *Patient population.* The relevant clinical, electrocardiographic and echocardiographic  
215 characteristics of the patients are shown in Table 1. There was no association between ECG  
216 P-wave duration, left atrial diameter, and any physiological or immunohistochemical  
217 parameter.

218 *TABLE 1 NEAR HERE*

219

220 *Specimens.* Biopsy samples were of sufficient size to perform impedance measurements for  
221 all patients (n=23). However, connexin quantification by Western blot analysis was only  
222 possible in 20/23 samples. Fibrosis quantification and morphometry was performed in 16/23  
223 samples and intercalated disc area and Cx40 gap junction protein per area *en-face* disc were  
224 measured in 12/23 patients.

225

226 *Connexin expression and myocardial resistivity.* Table 2 shows values of physiological and  
227 histological parameters for each patient. Figures 2A and B show plots of right atrial Cx40 and  
228 Cx43 expression against corresponding  $R_i$  and  $R_j$  values. There were significant positive  
229 correlations between Cx40 expression and  $R_i$ , ( $r=0.64$ ,  $p<0.01$ ,  $n=20$ ) as well as  $R_j$ , ( $r=0.63$ ,  
230  $p=0.01$ ,  $n=20$ ). Cx43 expression, however, did not correlate with either  $R_i$  or  $R_j$  and there  
231 was no correlation between either connexin or  $R_c$  (not shown). There was also a significant  
232 positive correlation between the proportional level of Cx40 expression ( $Cx40/[Cx40+Cx43]$ )  
233 and both  $R_i$  ( $r=0.58$ ,  $p<0.01$ ,  $n=20$ ) and  $R_j$  ( $r=0.51$ ,  $p=0.02$ ,  $n=20$ ), (Figure 2C).

234 *FIGURE 2 TABLE 2 NEAR HERE*

235

236 *Cellular connexin distribution.* Figure 3A and 3B shows immunolabelling for Cx40 and Cx43  
237 respectively. Cx43 labelling was well distributed throughout all specimens but Cx40  
238 distribution was heterogeneous and patchy, with some regions intensely labelled and some

239 regions displaying less intense labelling, as described previously.<sup>8:14</sup> Both connexins were  
240 located predominantly at the intercalated discs at the poles of the myocytes but there was  
241 presence of labelling at the lateral cell borders of all specimens. A semi-quantative method  
242 was used to grade connexin localisation ranging from being confined exclusively to the  
243 normal, transversely orientated clusters at cell abutments (score 1), to a distribution of  
244 labelling within longitudinal arrays along the length of the myocyte, with markedly  
245 diminished labelling at the end-on abutments (score 5). The mean score was  $2.5 \pm 1$   
246 indicating a degree of lateralisation in all samples. Figure 3D shows that there was no  
247 association between Cx43 lateralisation score and  $R_j$  for each patient.

248 *FIGURE 3 NEAR HERE*

249

250 *Immunolabelled Cx40 gap junction protein per unit area of en-face disk and Cx40*  
251 *heterogeneity.* Given the relationship established between Cx40 expression and  $R_j$ , it was of  
252 interest to examine whether  $R_j$  was related to Cx40 expression specifically at the intercalated  
253 disc. Figure 3C shows enface views of a typical *en-face* intercalated disc. As described in the  
254 methods section, the quantity of Cx40 immunolabelled pixels were measured and expressed  
255 as a percentage of the area of the *en-face* disk. The mean intercalated disc area was  $96 \pm 37.8$   
256  $\mu\text{m}^2$ , mean Cx40 area was  $39.4 \pm 10.2 \mu\text{m}^2$ , and mean Cx40 gap junction area per *en-face*  
257 disk was  $45 \pm 20\%$ . Cx40 expression, measured by Western Blot analysis, did not  
258 significantly correlate with Cx40 gap junction per unit area of enface disc ( $p=\text{NS}$ ,  $n=12$ )  
259 (Figure 4A), but there was a significant positive correlation between Cx40 gap junction per  
260 unit area of *en-face* disc and  $R_j$ , ( $r=0.66$ ,  $p=0.02$ ,  $n=12$ ) (Figure 4B). The heterogeneity of  
261 Cx40 labelling, was examined by assessing the percentage of labelled cells per field for 12/23  
262 patients, and values are shown in table 2. There was no significant relationship between Cx40  
263 heterogeneity and junctional resistivity ( $r= -0.44$   $p=\text{NS}$ ) (Figure 4C).

264

265 *FIGURE 4 NEAR HERE*

266

267 *The relationships between age, connexin expression and myocardial resistivity.* There was a  
268 significantly positive correlation between advancing age and both  $R_i$  ( $r= 0.77$ ,  $p<0.0001$ ) and  
269  $R_j$  ( $r= 0.65$ ,  $p<0.001$ ,  $n=23$ ) (Figure 5A), and a corresponding correlation between age and  
270 Cx40 expression ( $r=0.54$ ,  $p=0.01$ ,  $n=20$ ) (Figure 5B), but not Cx43 expression. There was no  
271 relationship between age and  $R_c$  (not shown).

272

273 Myocardial fibrosis was quantified for 16/23 patient samples to provide average values from  
274 six randomly selected fields. There was no significant relationship between age and the  
275 percentage of myocardial fibrosis (Figure 5C). Advancing age was associated with an  
276 increase in Cx40 gap junction protein per unit area *en-face* disk ( $r=0.61$ ,  $p=0.02$ ,  $n=12$ )  
277 (Figure 5D) but not with Cx43 area or lateralisation score (Figure 5E).

278

279

280 *FIGURE 5 NEAR HERE*

281

282

283

284 **Discussion**

285 The main findings of this study are that increased Cx40 expression, and an increase in the  
286 relative expression of Cx40 (Cx40/[Cx40+Cx43]), are associated with an increase in  
287 myocardial resistivity in the human right atrium, that it is the Cx40 specifically located in the  
288 intercalated disk which correlates with gap junctional resistivity, and that increased atrial  
289 myocardial resistivity with advancing age is associated with an increase in Cx40 expression.

290 On the background of our previous demonstration of a relationship between atrial connexin  
291 expression and conduction velocity measured in vivo in the human right atrium,<sup>8</sup> we now  
292 confirm a relationship between atrial connexin expression and directly measured gap junction  
293 resistivity in multicellular human right atrial preparations.

294

295 *Connexin40 expression and atrial resistivity.* Connexin-knockout mice have been shown to  
296 have changes in conduction velocity in atrial myocardium<sup>7</sup> and in the specialised conduction  
297 system<sup>15</sup> providing evidence that connexins are a key determinant of impulse propagation.  
298 However, by contrast with the present study, murine Cx-gene knock-out models have  
299 indicated that reduction of Cx40 slows atrial conduction with corresponding prolongation of  
300 the P-wave on the ECG.<sup>5-7</sup> Further, we previously demonstrated an inverse relationship  
301 between human right atrial Cx40 expression and CV, measured in open-chested mapping  
302 studies of patients undergoing cardiac surgery.<sup>8</sup> Given that CV is determined by several  
303 factors including gap-junctional coupling,<sup>16</sup> depolarising currents,<sup>17</sup> and tissue architecture,<sup>18</sup>  
304 it is an important finding of the current study that the inverse relationship between Cx40  
305 expression and CV is mediated by an increase in atrial gap junction resistivity. Indeed, given  
306 that the unitary conductance of pure Cx40 channels is higher than that of pure Cx43 and  
307 Cx45 channels,<sup>19;20</sup> it might be expected that with the naturally occurring variations in Cx40

308 expression in the human heart, a higher level of Cx40 expression would result in a lower  
309 myocardial resistivity.

310 However, when a pair of myocytes expresses two or more connexins channels the different  
311 potential combinations of connexins (homomeric homotypic, homomeric heterotypic,  
312 heteromeric homotypic or heteromeric heterotypic),<sup>21;22</sup> result in a corresponding variety of  
313 functional properties of the gap-junctional channels. In-vitro studies have confirmed that  
314 Cx40 and Cx43 interact in the formation of heteromeric/heterotypic gap junction channels,<sup>23</sup>  
315 and we have previously confirmed co-localisation of Cx40 and Cx43 within human right  
316 atrial gap junction plaques,<sup>8</sup> although co-localisation does not prove that Cx40 and Cx43  
317 form mixed channels. Cells which co-express Cx40 and Cx43<sup>23-25</sup> are known to be more  
318 susceptible to uncoupling than cells expressing a single connexin type.<sup>25</sup> Therefore an  
319 increase in Cx40 expression may result in the formation of either non-functional or low  
320 conductance channels, which result in an increase in overall gap junctional resistivity. It is  
321 also possible that an alteration of right atrial Cx40 expression may somehow alter Cx43  
322 function. A study of cultured atrial myocytes with heterozygous (Cx40<sup>+/-</sup> or Cx43<sup>+/-</sup>) or  
323 suppressed (Cx40<sup>-/-</sup> or Cx43<sup>-/-</sup>) connexin expression showed that reduced Cx40 expression  
324 was associated with increased CV and also increased Cx43 labelling in gap junctions.<sup>9</sup>  
325 However, a study of cultured murine Cx43 ablated cells (Cx43<sup>-/-</sup>) demonstrated that ablation  
326 of Cx43 reduced electrical conductance between myocytes as well as the expression of Cx40  
327 and Cx45.<sup>25a</sup> Furthermore, a study of the effects of a novel frameshift Cx43 mutation discovered in  
328 man, on murine cultured cells, confirmed a reduction of Cx40 gap junction conductance  
329 thought due to abnormal connexin protein trafficking to the intercalated disc,<sup>25b</sup> These  
330 studies highlight the fact that interactions between co-expressed connexins are not  
331 straightforward and predictable, and therefore the functional consequences of altered

332 connexin expression associated with age or disease states such as atrial fibrillation, may not  
333 be predictable from simple measurement of connexin quantity alone.

334 We did not observe a direct relationship between the quantity of Cx43 expression and  $R_j$ .  
335 However it remains possible that Cx43 may influence on  $R_j$  in a manner not identified by our  
336 current techniques.

337

338 *Advancing age, atrial connexins and resistivity.* We,<sup>26</sup> and others,<sup>27</sup> have shown an age-  
339 associated slowing of right atrial CV in human endocardial mapping studies although the  
340 mechanism underlying this phenomenon remains unknown. Animal studies have confirmed  
341 that atrial fibrosis with advancing age is associated with conduction slowing and increased  
342 rate of arrhythmogenesis,<sup>28:29</sup> and human studies have demonstrated a correlation between  
343 levels of atrial fibrosis and advancing age<sup>29a, 29b</sup>. We previously have shown that human  
344 atrial CV did not directly correlate with endomysial connective tissue content,<sup>8</sup> we did not  
345 find any association between age and quantity of myocardial connective tissue in this present  
346 study. A finding similar to previous reports.<sup>29c, 29d</sup> It remains possible, however, that the  
347 pattern of connective tissue deposition in older humans may change and result in greater  
348 separation of atrial bundles.<sup>30</sup> Our present study instead demonstrated an age associated  
349 increase in Cx40 expression, Cx40 gap junction protein per unit area of enface cells, and  $R_j$ .  
350 There have been no previous functional studies of the effects of ageing on cardiac gap  
351 junctions in the human atrium. However, a study of the effects of ageing on canine atrial  
352 myocardium,<sup>31</sup> comparing young (6-12 months) and older (6-10 years) dogs, demonstrated  
353 that gap junction distribution became progressively more polarized with increasing age and  
354 localized to the cell termini. There was no change in the cellular distribution of gap junctions  
355 in the human right atrium with advancing age in our present study, although the area of Cx40  
356 gap junction protein per unit area of *en-face* disk increased with advancing age.

357

358 *Insights from correlations of connexin expression with junctional resistivity.* Cx43 quantity,  
359 measured by immunofluorescence, has been previously correlated with direct measurements  
360 of intercellular electrical conductance (the inverse of resistivity) in engineered rat myocytes.<sup>32</sup>  
361 Our study now provides a unique insight into human connexin biology, in particular the  
362 importance of Cx40 in determining atrial resistivity, and the effects of aging on atrial  
363 connexin expression and resistivity. Our results may also explain the finding that increased  
364 right atrial Cx40 expression in sinus rhythm is a predictor of the risk of developing post-  
365 operative AF,<sup>14</sup> and that an up-regulation of right atrial Cx40 has been described in  
366 association with atrial fibrillation in man.<sup>33</sup> However, although little is currently known about  
367 the mechanisms that underlie age-related atrial remodelling, or the control mechanisms or  
368 modulators of Cx40 expression, in the era of pharmacological<sup>34</sup> and genetic modulation<sup>35</sup> of  
369 connexin expression, human atrial Cx40 expression may be a potential therapeutic target in  
370 the prevention of atrial arrhythmias.

### 371 **Limitations**

372 Specimens were of insufficient size to perform immunohistochemical experiments for all  
373 patients. Tissue was only collected from the atrial appendages and it is possible that the gap  
374 junction remodelling described in this paper is limited to the appendage only and not  
375 reflective to changes in other atrial regions. It is possible that the pre-operative medication  
376 taken by patients in this study could have influenced gap junction conductance. Although our  
377 results demonstrate an association between Cx40 expression, gap junction resistivity and  
378 advancing age they not prove a direct causality between these variables.

### 379 **Conclusion**



380 In the human right atrium, Cx40 expression and Cx40 gap junction protein per unit area of  
381 *en-face* disks, are directly related to gap junctional resistivity. Advancing age is associated  
382 with an increase in Cx40 expression and gap junction resistivity, and these findings may  
383 explain the association of advancing age with atrial arrhythmias.

384

#### 385 **Acknowledgements**

386 Microscopy was performed in the Facility for Imaging by Light Microscopy (FILM) at  
387 Imperial College London.

388

#### 389 **Funding Sources**

390 This study is supported by funding awarded by the British Heart Foundation  
391 (FS/03/031/15498 and RG/05/009).

#### 392 **Disclosures**

393 None

## References

- (1) Harris AL. Emerging issues of connexin channels: biophysics fills the gap. *Q Rev Biophys.* 2001; 34(3):325-472.
- (2) Kanno S, Saffitz JE. The role of myocardial gap junctions in electrical conduction and arrhythmogenesis. *Cardiovasc Pathol.* 2001; 10(4):169-177.
- (3) Willecke K, Eiberger J, Degen J, Eckardt D, Romualdi A, Guldenagel M, Deutsch U, Söhl G. Structural and functional diversity of connexin genes in the mouse and human genome. *Biol Chem.* 2002; 383(5):725-737.
- (4) Vozzi C, Dupont E, Coppens SR, Yeh HI, Severs NJ. Chamber-related differences in connexin expression in the human heart. *J Mol Cell Cardiol.* 1999; 31(5):991-1003.
- (5) Bagwe S, Berenfeld O, Vaidya D, Morley GE, Jalife J. Altered right atrial excitation and propagation in connexin40 knockout mice. *Circulation.* 2005; 112(15):2245-2253.
- (6) Eckardt D, Theis M, Degen J, Ott T, van Rijen HV, Kirchhoff S, Kim JS, de Bakker JM, Willecke K. Functional role of connexin43 gap junction channels in adult mouse heart assessed by inducible gene deletion. *J Mol Cell Cardiol.* 2004; 36(1):101-110.
- (7) Thomas SA, Schuessler RB, Berul CI, Beardslee MA, Beyer EC, Mendelsohn ME, Saffitz JE. Disparate effects of deficient expression of connexin43 on atrial and ventricular conduction: evidence for chamber-specific molecular determinants of conduction. *Circulation.* 1998; 97(7):686-691.

- (8) Kanagaratnam P, Rothery S, Patel P, Severs NJ, Peters NS. Relative expression of immunolocalized connexins 40 and 43 correlates with human atrial conduction properties. *J Am Coll Cardiol.* 2002; 39(1):116-123.
- (9) Beauchamp P, Yamada KA, Baertschi AJ, Green K, Kanter EM, Saffitz JE, Kléber AG. Relative contributions of connexins 40 and 43 to atrial impulse propagation in synthetic strands of neonatal and fetal murine cardiomyocytes. *Circ Res.* 2006; 99(11):1216-1224.
- (10) Jongsma HJ, Wilders R. Gap junctions in cardiovascular disease. *Circ Res.* 2000; 86(12):1193-1197.
- (11) Cooklin M, Wallis WR, Sheridan DJ, Fry CH. Changes in cell-to-cell electrical coupling associated with left ventricular hypertrophy. *Circ Res.* 1997; 80(6):765-771.
- (11a) Fry CH, Salvage SC, Manazza A, Dupont E, Labeed FH, Hughes MP, Jabr RI. Cytoplasm resistivity of mammalian atrial myocardium determined by dielectrophoresis and impedance methods. *Biophys J.* 2012 Dec 5;103(11):2287-2294.
- (12) Patel PM, Plotnikov A, Kanagaratnam P, Shvilkin A, Sheehan CT, Xiong W, Danilo P Jr, Rosen MR, Peters NS. Altering ventricular activation remodels gap junction distribution in canine heart. *J Cardiovasc Electrophysiol.* 2001; 12(5):570-577.
- (13) Fitzmaurice M, Bordagaray JO, Engelmann GL, Richards-Kortum R, Kolubayev T, Feld MS, Ratliff NB, Kramer JR. Argon ion laser-excited autofluorescence in normal and atherosclerotic aorta and coronary arteries: morphologic studies. *Am Heart J.* 1989; 118(5 Pt 1):1028-1038.

- (14) Dupont E, Ko Y, Rothery S, Coppens SR, Baghai M, Haw M, Severs NJ. The gap-junctional protein connexin40 is elevated in patients susceptible to postoperative atrial fibrillation. *Circulation*. 2001; 103(6):842-849.
- (15) van Rijen HV, van Veen TA, van Kempen MJ, Wilms-Schopman FJ, Potse M, Krueger O, Willecke K, Opthof T, Jongsma HJ, de Bakker JM. Impaired conduction in the bundle branches of mouse hearts lacking the gap junction protein connexin40. *Circulation*. 2001; 103(11):1591-1598.
- (16) Rohr S, Kucera JP, Fast VG, Kléber AG. Paradoxical improvement of impulse conduction in cardiac tissue by partial cellular uncoupling. *Science*. 1997; 275(5301):841-844.
- (17) Cranefield PF, Wit AL, Hoffman BF. Conduction of the cardiac impulse. 3. Characteristics of very slow conduction. *J Gen Physiol*. 1972; 59(2):227-246.
- (18) Kucera JP, Kléber AG, Rohr S. Slow conduction in cardiac tissue, II: effects of branching tissue geometry. *Circ Res*. 1998; 83(8):795-805.
- (19) Bukauskas FF, Elfgang C, Willecke K, Weingart R. Biophysical properties of gap junction channels formed by mouse connexin40 in induced pairs of transfected human HeLa cells. *Biophys J*. 1995; 68(6):2289-2298.
- (20) Veenstra RD, Wang HZ, Beblo DA, Chilton MG, Harris AL, Beyer EC, Brink PR. Selectivity of connexin-specific gap junctions does not correlate with channel conductance. *Circ Res*. 1995; 77(6):1156-1165.
- (21) Kumar NM. Molecular biology of the interactions between connexins. *Novartis Found Symp* 1999; 219:6-16.

- (22) White TW, Bruzzone R. Multiple connexin proteins in single intercellular channels: connexin compatibility and functional consequences. *J Bioenerg Biomembr.* 1996; 28(4):339-350.
- (23) Valiunas V, Gemel J, Brink PR, Beyer EC. Gap junction channels formed by coexpressed connexin40 and connexin43. *Am J Physiol Heart Circ Physiol.* 2001; 281(4):H1675-H1689.
- (24) He DS, Jiang JX, Taffet SM, Burt JM. Formation of heteromeric gap junction channels by connexins 40 and 43 in vascular smooth muscle cells. *Proc Natl Acad Sci U SA.* 1999; 96(11):6495-6500.
- (25) He DS, Burt JM. Mechanism and selectivity of the effects of halothane on gap junction channel function. *Circ Res.* 2000; 86(11):E104-E109.
- (25a) Desplantez T, McCain ML, Beauchamp P, Rigoli G, Rothen-Rutishauser B, Parker KK, Kleber AG. [Connexin43 ablation in foetal atrial myocytes decreases electrical coupling, partner connexins, and sodium current.](#) *Cardiovasc Res.* 2012 Apr 1;94(1):58-65.
- (25b) Thibodeau IL, Xu J, Li Q, Liu G, Lam K, Veinot JP, Birnie DH, Jones DL, Krahn AD, Lemery R, Nicholson BJ, Gollob MH. [Paradigm of genetic mosaicism and lone atrial fibrillation: physiological characterization of a connexin 43-deletion mutant identified from atrial tissue.](#) *Circulation.* 2010 Jul 20;122(3):236-44.
- (26) Kojodjojo P, Kanagaratnam P, Markides V, Davies DW, Peters N. Age-related changes in human left and right atrial conduction. *J Cardiovasc Electrophysiol.* 2006; 17(2):120-127.

- (27) Kistler PM, Sanders P, Fynn SP, Stevenson IH, Spence SJ, Vohra JK, Sparks PB, Kalman JM. Electrophysiologic and electroanatomic changes in the human atrium associated with age. *J Am Coll Cardiol.* 2004; 44(1):109-116.
- (28) Anyukhovskiy EP, Sosunov EA, Plotnikov A, Gainullin RZ, Jhang JS, Marboe CC, Rosen MR. Cellular electrophysiologic properties of old canine atria provide a substrate for arrhythmogenesis. *Cardiovasc Res.* 2002; 54(2):462-469.
- (29) Hayashi H, Wang C, Miyauchi Y, Omichi C, Pak HN, Zhou S, Ohara T, Mandel WJ, Lin SF, Fishbein MC, Chen PS, Karagueuzian HS. Aging-related increase to inducible atrial fibrillation in the rat model. *J Cardiovasc Electrophysiol.* 2002; 13(8):801-808.
- (29a) Goette A, Juenemann G, Peters B, Klein HU, Roessner A, Huth C, Röcken C. [Determinants and consequences of atrial fibrosis in patients undergoing open heart surgery.](#) *Cardiovasc Res.* 2002;54(2):390-6.
- (29b) Gramley F, Lorenzen J, Knackstedt C, Rana OR, Saygili E, Frechen D, Stanzel S, Pezzella F, Koellensperger E, Weiss C, Münzel T, Schauerte P. [Age-related atrial fibrosis.](#) *Age.* 2009;31(1):27-38.
- (29c) Platonov PG, Mitrofanova LB, Orshanskaya V, Ho SY. Structural abnormalities in atrial walls are associated with presence and persistency of atrial fibrillation but not with age. *J Am Coll Cardiol.* 2011;58:2225–2232.
- (30) Spach MS, Dolber PC. Relating extracellular potentials and their derivatives to anisotropic propagation at a microscopic level in human cardiac muscle. Evidence for electrical uncoupling of side-to-side fiber connections with increasing age. *Circ Res.* 1986; 58(3):356-371.

- (31) Koura T, Hara M, Takeuchi S, Ota K, Okada Y, Miyoshi S, Watanabe A, Shiraiwa K, Mitamura H, Kodama I, Ogawa S. Anisotropic conduction properties in canine atria analyzed by high-resolution optical mapping: preferential direction of conduction block changes from longitudinal to transverse with increasing age. *Circulation*. 2002; 105(17):2092-2098.
- (32) McCain ML, Desplantez T, Geisse NA, Rothen-Rutishauser B, Oberer H, Parker KK, Kléber AG. Cell-to-cell coupling in engineered pairs of rat ventricular cardiomyocytes: relation between Cx43 immunofluorescence and intercellular electrical conductance. *Am J Physiol Heart Circ Physiol*. 2012; 302(2):H443-H450.
- (33) Polontchouk L, Haefliger JA, Ebelt B, Schaefer T, Stuhlmann D, Mehlhorn U, Kuhn-Regnier F, De Vivie ER, Dhein S. Effects of chronic atrial fibrillation on gap junction distribution in human and rat atria. *J Am Coll Cardiol*. 2001; 38(3):883-891.
- (34) Kjolbye AL, Haugan K, Hennan JK, Petersen JS. Pharmacological modulation of gap junction function with the novel compound rotigaptide: a promising new principle for prevention of arrhythmias. *Basic Clin Pharmacol Toxicol*. 2007; 101(4):215-230.
- (35) Igarashi T, Finet JE, Takeuchi A, Fujino Y, Strom M, Greener ID, Rosenbaum DS, Donahue JK. Connexin gene transfer preserves conduction velocity and prevents atrial fibrillation. *Circulation*. 2012; 125(2):216-225.

**Table 1** Patient characteristics.

Patient	Age (years)	Sex	Operation	History	Medication	LV EF (%)	LA (mm)	P-wave duration (s)
1	64	M	AVR	AS	BB	30	34	0.12
2	80	F	CABG AVR	IHD AR HT	CCB	30-40	45	0.12
3	54	F	AVR	AR	ARB	>50	44	0.12
4	69	M	CABG	IHD DM HT	BB CCB ACE	>50	40	0.08
5	53	M	CABG	IHD DM HT	CCB	>50	42	0.1
6	72	F	CABG	HT	BB ACE	>50	40	0.12
7	68	M	CABG	MI HT	BB ACE	40-50	38	0.12
8	78	F	CABG AVR	MI AS HT	BB CCB ACE	40-50	36	0.08
9	77	F	CABG	IHD	BB ACE	>50	30	0.12
10	75	M	CABG	MI HT	BB ACE	>50	45	0.08
11	65	F	CABG AVR	IHD AS DM	CCB ARB	>50	47	0.1
12	55	M	CABG	MI HT	BB ACE	40-50	42	0.08
13	67	M	CABG	MI HT	BB	>50	40	0.08
14	76	F	CABG AVR	AS AR		35-40	37	0.08
15	76	M	CABG	IHD	CCB	>50	41	0.12
16	68	M	CABG	MI DM HT	ACE CCB	>50	49	0.12
17	74	M	CABG	MI DM	BB ACE	35	39	0.08
18	72	M	CABG AVR	IHD AR	BB ACE	>50	31	0.12
19	73	M	CABG	MI	BB CCB ACE	>50	43	0.08
20	72	M	CABG	MI	BB	>50	40	0.16
21	60	M	CABG	IHD	BB ACE	>50	38	0.18
22	55	F	AVR	AS		>50	41	0.16
23	62	M	CABG	IHD	ACE	>50	33	0.12

LV EF = Left Ventricular Ejection Fraction; LA = Left Atrium; PWD = P wave duration;

CABG = Coronary Artery Bypass Grafting; AVR = Aortic Valve Replacement; MI =



Myocardial Infarction; IHD = Ischaemic Heart Disease; AS = Aortic Stenosis; AR = Aortic Regurgitation; HT = Hypertension; DM = Diabetes Mellitus; BB = Beta Blocker; CCB = Calcium Channel Blocker; ACE = Ace Inhibitor; ARB = Angiotensin Receptor Blocker.

Table 2 Physiological and histological parameters

Patient	$R_i(\Omega.cm)$	$R_c(\Omega.cm)$	$R_j(\Omega.cm)$	Cx43 units	Cx40 units	Fibrosis (%)	Cx40 area/disc (%)	Cx40 labelling per field (%)
1	320	194	126	110	78	N/A	N/A	N/A
2	375	230	145	103	114	N/A	N/A	N/A
3	303	227	76	22	N/A	N/A	N/A	N/A
4	397	208	189	21	170	31.6±12.4	36.0±10.9	74.0±10.0
5	329	173	156	24	80	N/A	N/A	N/A
6	404	216	188	94	151	39.4±12.6	35.7±10.7	86.4±11.0
7	344	225	119	117	48	32.1±15.5	34.5±14.4	80.6±8.6
8	474	182	292	104	150	33.0±13.9	N/A	N/A
9	420	181	239	29	202	19.4±9.9	49.6±16.32	83.1±12
10	443	154	289	30	146	52.0±12.8	N/A	N/A
11	402	225	177	11	121	51.0±10.9	23.9±7.8	85.4±8.1
12	291	178	113	100	100	26.2±12.1	36.5±10.5	92.1±7.2
13	315	208	107	104	34	73.7±20.9	N/A	N/A
14	456	218	238	10	210	56.7±7.6	55.9±5.8	81.1±7.4
15	396	246	150	18	130	34.2±22.4	N/A	N/A
16	426	165	261	86	102	18.8±7.1	51.2±9.7	80.6±6.4
17	488	227	261	25	96	42.1±29.6	57.0±9.7	87.6±5.0
18	467	213	254	42	152	21.8±3.5	51.3±10.0	80.8±8.3
19	386	183	180	138	106	35.3±16.1	56.1±12.1	80.9±7.0
20	497	182	315	99	109	27.7±9.3	56.4±15.3	74.1±10.1
21	290	199	91	N/A	N/A	N/A	N/A	N/A
22	265	158	107	N/A	N/A	N/A	N/A	N/A
23	356	237	119	53	66	N/A	N/A	N/A

$R_i$  = Intracellular resistivity;  $R_j$  = Gap junction resistivity;  $R_c$  = Sarcoplasmic resistivity;

## **Figure Legends**

Figure 1. A plot of intracellular resistance,  $R_i$ , as a function of measuring frequency. The dotted lines represent the frequency-independent values of  $R_i$  at high and low frequencies. The smaller value at high frequency corresponds to cytoplasmic resistivity,  $R_c$ ; the difference between the two values is a function of gap junction resistance,  $R_j$ .

Figure 2. The relationship between Cx40 and Cx43 expression, as well as relative Cx ratio ( $Cx40/Cx40+Cx43$ ), with  $R_i$  (open symbols) and  $R_j$  (closed symbols). A, Increasing Cx40 expression was significantly associated with both  $R_i/R_j$  ( $p<0.01$  and  $p=0.01$  respectively). B, Cx43 expression did not correlate with  $R_i/R_j$ . C, The relative Cx ratio ( $Cx40/Cx40 +Cx43$ ) was significantly associated with to  $R_i/R_j$  ( $p<0.01$  and  $p=0.02$  respectively).

Figure 3. A and B, Cx40 (A) and Cx43 (B) immunolabelling showing predominant labeling at the intercalated discs at the poles of the cells. White arrows indicate cell alignment along longitudinal axis and white bar = 25  $\mu\text{m}$ . C, Cx40 immunolabelling of enface discs allowing measurement of Cx40 area in each disc (white bar = 10  $\mu\text{m}$ ). D, A plot of gap junctional resistivity,  $R_j$ , against Cx43 lateralization score ( $p=\text{NS}$ ).

Figure 4. Plots of Cx40 gap junction per unit area of *en-face* disk and: A, Cx40 expression determined by Western Blot analysis ( $p=\text{NS}$ ); and B, gap junctional resistivity ( $p=0.02$ ). C, plot of  $R_j$  against Cx40 heterogeneity measured in percentage of labeled cells per field.

Figure 5. Plots of age against: A,  $R_i$  (open symbol) and  $R_j$  (closed symbol) ( $p<0.001$  and  $p<0.01$  respectively); B, Cx40 expression ( $p=0.01$ ); C, percentage fibrosis per field ( $p=\text{NS}$ ); D, Cx40 gap junction protein per unit area of *en-face* disk ( $p=0.03$ ); and E, Cx43 lateralisation score ( $p=\text{NS}$ ).

Figure 1

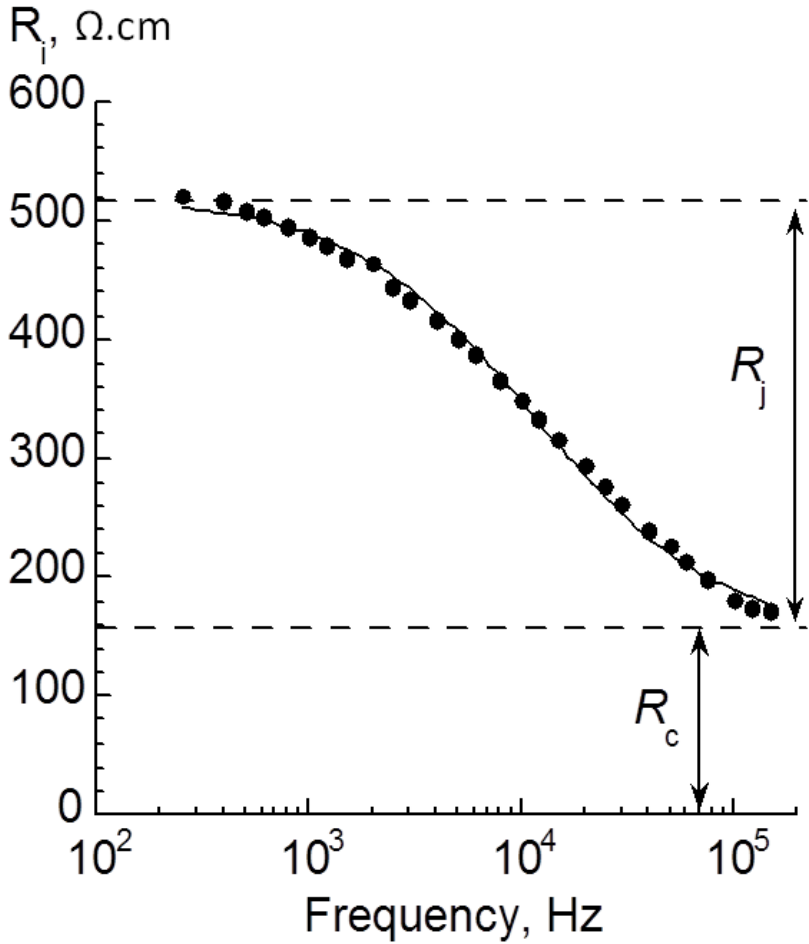
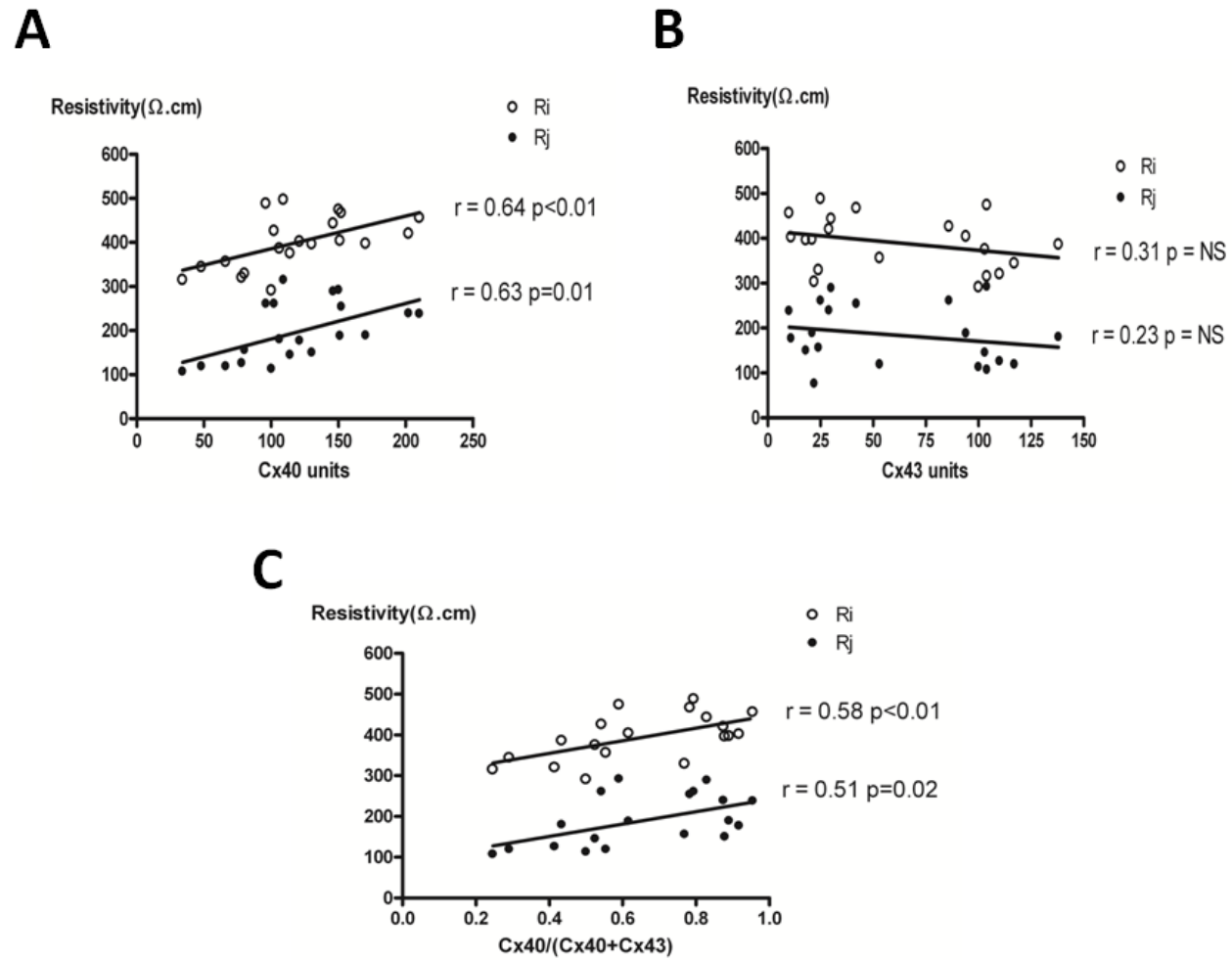


Figure 2



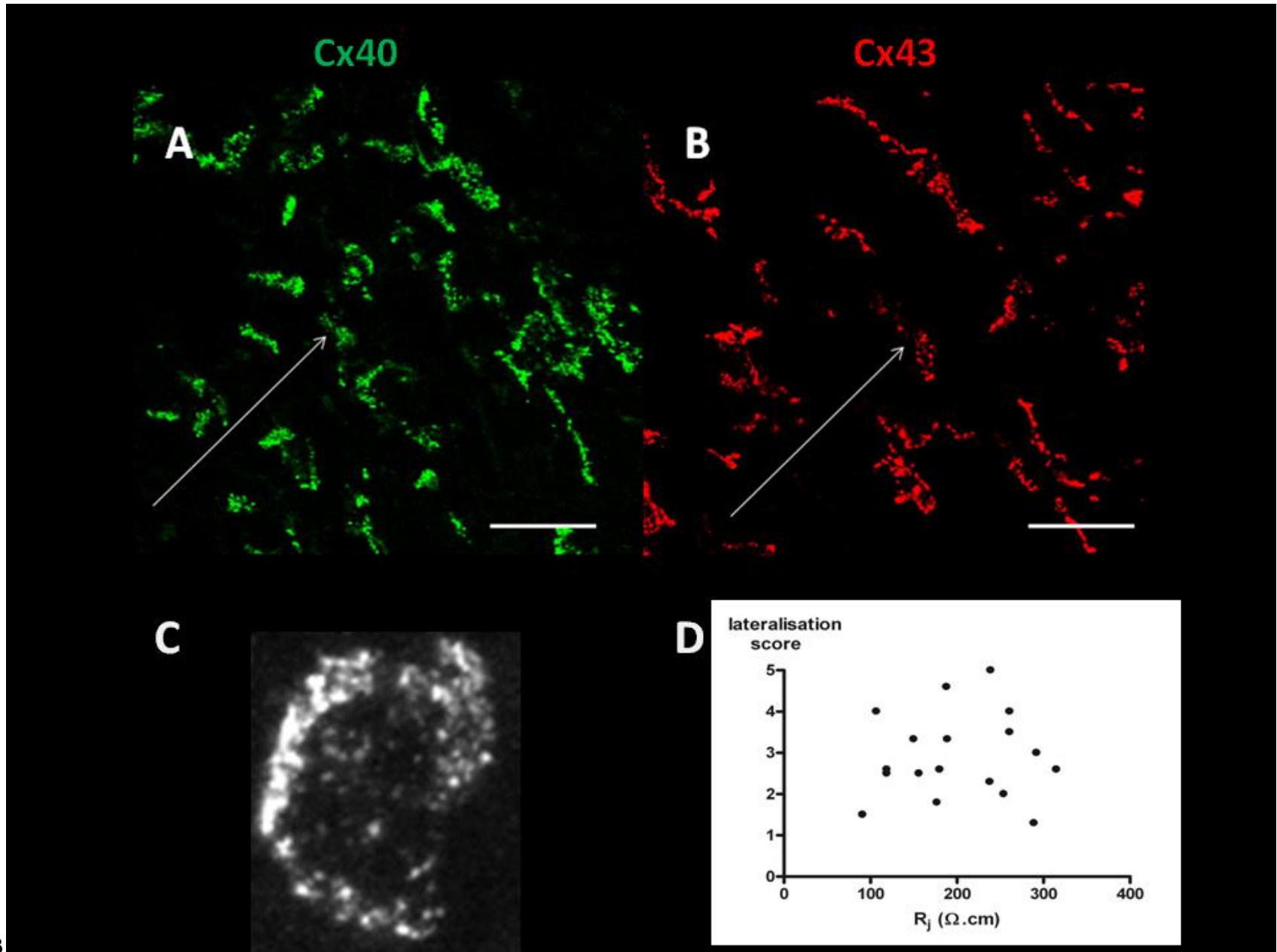


Figure 3





**Figure 5**

